

Received: 15 October 2007,

Revised: 13 November 2007,

Accepted: 14 November 2007,

Published online in Wiley InterScience: 9 January 2008

(www.interscience.wiley.com) DOI 10.1002/poc.1310

# Synthesis and thermolysis of Diels–Alder adducts of 2,9-dialkylpentacenes with diethyl azodicarboxylate

Kazuo Okamoto<sup>a</sup>, Kouta Shiodera<sup>a</sup>, Takumi Kawamura<sup>a</sup> and Kenji Ogino<sup>a\*</sup>

A series of Diels–Alder adducts of 2,9-dialkylpentacenes with diethyl azodicarboxylate were synthesized, and their thermolysis behaviors or retro-Diels–Alder reactions to regenerate dialkylpentacene were investigated via thermogravimetric analysis, IR and UV–Vis spectroscopy. Synthesized Diels–Alder adducts or precursors formed stable molecular glass. The transparent films on glass slide or silicon wafer were easily fabricated by cast or spin-coating process. The precursors were smoothly converted to corresponding dialkylpentacenes by heating at 300°C. The domain size of regenerated dialkylpentacenes was in the range of 50–200 μm. Copyright © 2008 John Wiley & Sons, Ltd.

**Keywords:** Diels–Alder adduct; retro-Diels–Alder reaction; 2,9-dialkylpentacene; molecular glass

## INTRODUCTION

Organic thin field-effect transistors (OTFTs) are of great interest because of their potential to fabricate the low-cost, large-area, and flexible electronic devices. As semiconducting molecules, pentacene is one of the most popular and promising aromatic compounds in the OTFT applications since it offers high performance such as higher mobility and better on-off ratio similar to those of amorphous silicon TFTs.<sup>[1]</sup> However non-substituted pentacene has the drawback for the application of solution process since it is essentially insoluble in organic solvents at room temperature.<sup>[2]</sup> In the fabrication of OTFTs, wet-processes like an ink-jet printing, spin-coating, and bar-coating are strongly desirable to meet the demands. Therefore it is of importance to design semiconducting molecules applicable to solution processes.

There are mainly two strategies for the molecular design. One is the introduction of substituents on pentacene ring in order to improve the solubility. Although the substituents generally disturb the molecular packing leading to poor OTFT performance, precise molecular design, however, enabled the appropriately ordered molecular packing for higher mobility and performance in OTFTs.<sup>[3,4]</sup>

The utilization of soluble precursors based on pentacene is the alternative method, in which thin films have been fabricated with soluble precursor followed by the conversion to pentacene.<sup>[5–10]</sup> Mainly Diels–Alder adducts have been reported as precursors, since Diels–Alder adducts show higher solubility and excellent air stability and are easily converted to pentacene via retro-Diels–Alder reaction.<sup>[8–10]</sup> Several dienophiles have been used for this purpose, including alkyl azodicarboxylate<sup>[8]</sup> and *N*-sulfinylamides.<sup>[9,10]</sup> Among them alkyl azodicarboxylates are commercially available and relatively stable. Moreover resulting Diels–Alder adduct with pentacene, azapentacene derivative shows high solubility in organic solvent.<sup>[8]</sup>

Concerned with alkyl-substituted pentacenes, we originally reported that 2,9-dialkylpentacenes showed smectic phase when the alkyl chain was longer than C4.<sup>[11]</sup> Self-assembled properties of

liquid crystalline compounds have a potential for high performance OTFT in the solution process. Indeed the substituted hexabenzocoronenes (HBCs), which can be processed from solution to form films that are supermolecularly ordered columnar stacks lying parallel to the substrate, were applied to OTFT device.<sup>[12]</sup> Liquid crystalline terthiophene derivatives could be processed into self-assembled monodomain films.<sup>[13]</sup> Polymeric liquid crystalline materials have also been reported.<sup>[14–16]</sup> Although the solubility of 2,9-dialkylpentacene was better than that of pentacene, it is difficult to apply these derivatives to the OTFTs via solution processes owing to the lack of air stability of these derivatives in solution.

In this study, we synthesized a series of azapentacene derivatives via Diels–Alder reaction of 2,9-dialkylpentacenes with diethyl azodicarboxylate, and investigated their thermolysis behaviors. We believe that the combination of precursor film formation followed by conversion to 2,9-dialkylpentacene and the controlling molecular ordering or morphology utilizing its liquid crystallinity afford an OTFT device with high performance in the wet process, which is comparable to that fabricated with the dry process.

## RESULTS AND DISCUSSION

### Synthesis and characterization of precursors

A series of dialkylpentacenes were reacted with diethyl azodicarboxylate in toluene in order to produce Diels–Alder adducts or precursors as shown in Figure 1. <sup>1</sup>H-NMR and IR

\* Graduate School of Bio-Applications and Systems Engineering, Tokyo University of Agriculture and Technology, Koganei, Tokyo 184-8588, Japan.  
E-mail: kogino@cc.tuat.ac.jp

a K. Okamoto, K. Shiodera, T. Kawamura, K. Ogino  
Graduate School of Bio-Applications and Systems Engineering, Tokyo University of Agriculture and Technology, Koganei, Tokyo 184-8588, Japan

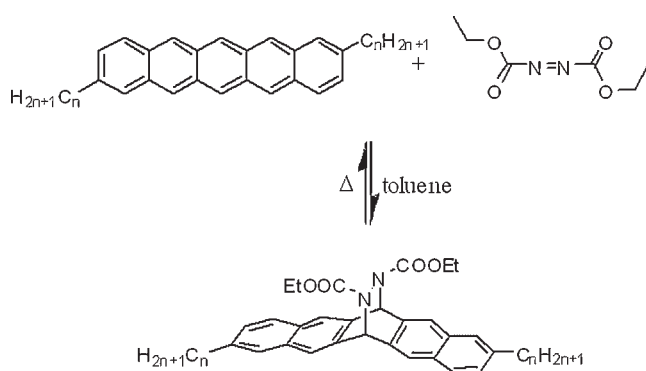


Figure 1. Synthetic route of Diels–Alder adducts for 2,9-dialkylpentacenes

spectra confirmed the successful synthesis of desired products. In  $^1\text{H}$ -NMR spectra of adducts, methyl proton in the ester group appeared as a broad signal in all cases. This is probably due to the hindered rotation about the  $N$ -COOEt bond as reported in the literature.<sup>[17]</sup> In UV-Vis spectra, characteristic five absorptions around 430, 466, 500, 537, and 582 nm observed in 2,9-dialkylpentacenes solution completely disappeared after the reaction.

Solubility of Diels–Alder adducts is dramatically increased compared with the corresponding dialkylpentacenes. They are almost miscible with toluene and chloroform. Although the solutions of 2,9-dialkylpentacenes were rather unstable and were bleached within 30 min when exposed to air and/or light,<sup>[11]</sup> no chemical changes were observed for Diels–Alder adducts during purification and storage processes. According to the literature,<sup>[10]</sup> Lewis acid catalyzed Diels–Alder reactions of 2,9-dialkylpentacenes with  $N$ -sulfinylacetamide were also carried out. It was revealed that resulting compounds were viscose liquid, and lacked storage stability since the color was changed from orange to purple due to retro-Diels–Alder reaction in a day at room temperature.

From DSC measurements, resulting compounds show only glass transition in the range from  $-8.6$  to  $90.1^\circ\text{C}$  dependent on the alkyl length, indicating that the precursor forms stable molecular glass. No crystallization was observed in the examined temperature range ( $-50$ – $200^\circ\text{C}$ ). Indeed spin-coating or cast methods of precursor solution afforded optical quality of transparent films.

Figure 2 shows MS spectrum of the Diels–Alder adduct (a) and 2,9-dihexylpentacene (b). In Fig. 2a, a peak at  $620\text{ m/z}$  was from the precursor, and the strongest peak was detected at  $446\text{ m/z}$ , which is in good agreement with the molecular weight of 2,9-dihexylpentacene, and the other main peaks were assigned as shown in Fig. 2a, and the fragmentation pattern of precursor is similar to that of 2,9-dihexylpentacene (as shown in Fig. 2b). These results suggest that the precursors can be easily converted to dialkylpentacene by the retro-Diels–Alder reaction. During the ionization process in MS measurements, samples were heated up to  $350^\circ\text{C}$ .

### Conversion behavior

Thermal behaviors for all pentacene precursors synthesized in this study were characterized with thermogravimetric (TG) analysis by monitoring weight loss accompanied with retro-Diels–Alder reaction. Figure 3a shows the TG analysis graph for 2,9-dihexylpentacene adduct in nitrogen atmosphere at normal pressure. Two steps weight loss curve was observed. The first and second steps were in the regions of  $300$  and  $430^\circ\text{C}$ , respectively. The second step was due to the decomposition and/or sublimation of 2,9-dihexylpentacene, as shown in Fig. 3b. The first step decomposition is considered to be caused via retro-Diels–Alder reaction. The first weight loss of  $24\%$  in the nitrogen atmosphere was almost in accordance with that caused by the elimination of diethyl azodicarboxylate from the precursor (theoretical value;  $28\%$ ). The total weight loss (about  $68\%$ ) was not consistent with that of pentacene. If decomposition and/or sublimation process

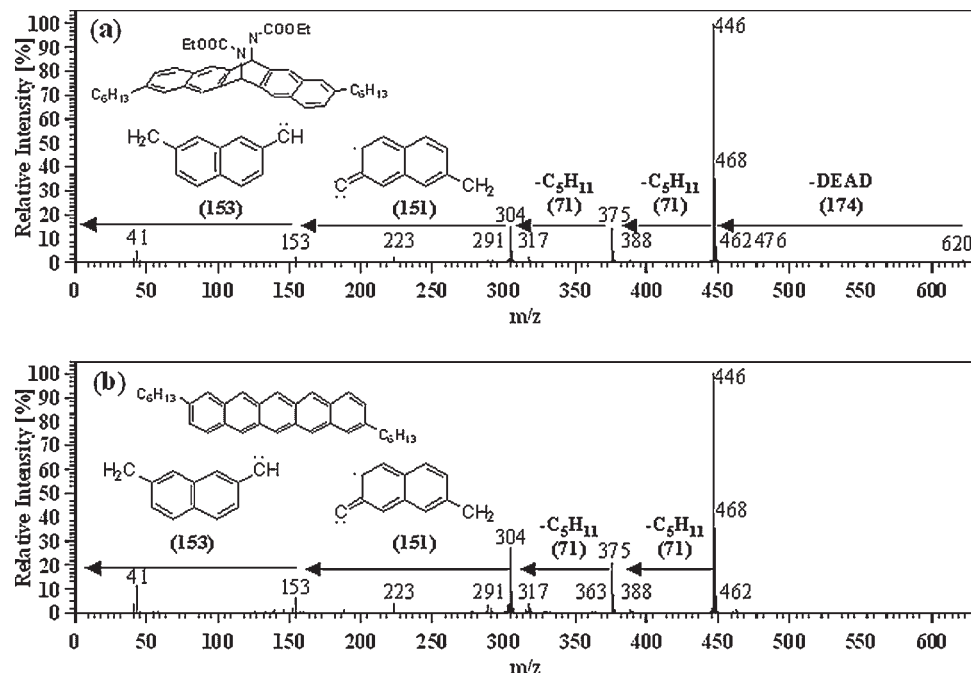
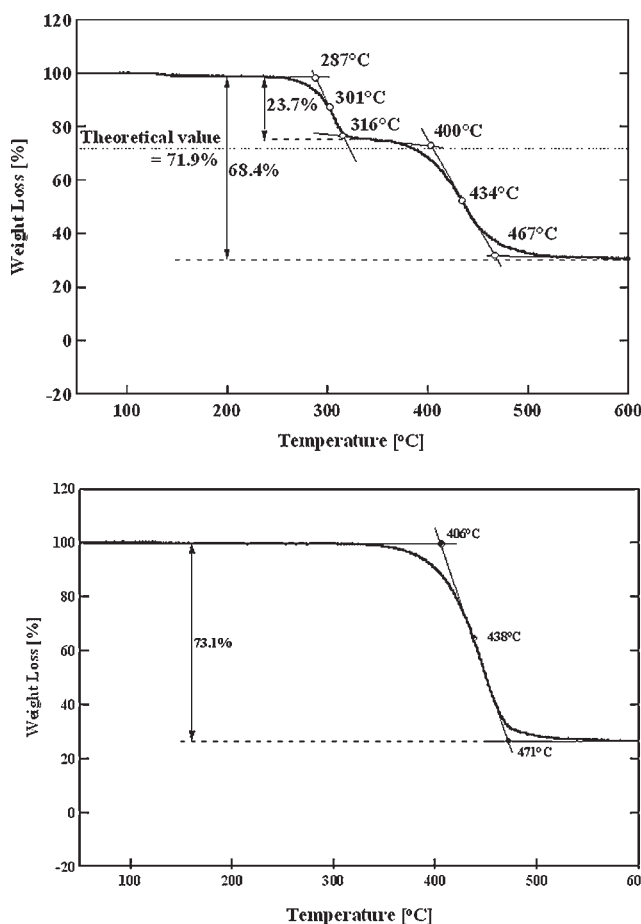


Figure 2. MS spectra of Diels–Alder adduct of 2,9-dihexylpentacene with diethyl azodicarboxylate (a) and of 2,9-dihexylpentacene (b)



**Figure 3.** Thermogravimetric analysis graphs for 2,9-dihexylpentacene precursor (a) and for 2,9-dihexylpentacene (b) in nitrogen atmosphere at normal pressure. Heating rate, 10°C/min

for regenerated 2,9-dihexylpentacene is the same as that for original dihexylpentacene, the total weight loss should be larger than 73.1%. The reason for inconsistency is hitherto unclear. The other precursors show almost the same thermal profiles as shown in Fig. 3a. In each case, the first step weight loss suggests that retro-Diels–Alder reaction smoothly occurs at around 300°C.

Figure 4 shows the dependence of the length of the dialkyl chain,  $n$ , for the dialkyl pentacene precursors on the conversion and decomposition temperatures. The conversion temperatures were almost constant (about 300°C) independent of the alkyl chain length. The slight odd–even effect was observed when the alkyl chain length  $n$  is 4–9, that is, homologue with even number of alkyl chain length showed the lower conversion temperature. As mentioned above 2,9-dialkylpentacenes show liquid crystallinity when  $n$  is over 4, and transition temperature from the crystal phase to the smectic phase showed similar odd–even effect.<sup>[11]</sup> It is considered that the packing process of resulting dialkylpentacenes has a slight effect on the retro-Diels–Alder process. In contrast, the decomposition temperatures increased with increase in the length of the alkyl,  $n$ .

As mentioned above, the glass transition temperatures monotonically decreased with increase in  $n$ , when  $n$  is until 10. There is no relationship between the glass transition temperature and conversion temperature. This is probably

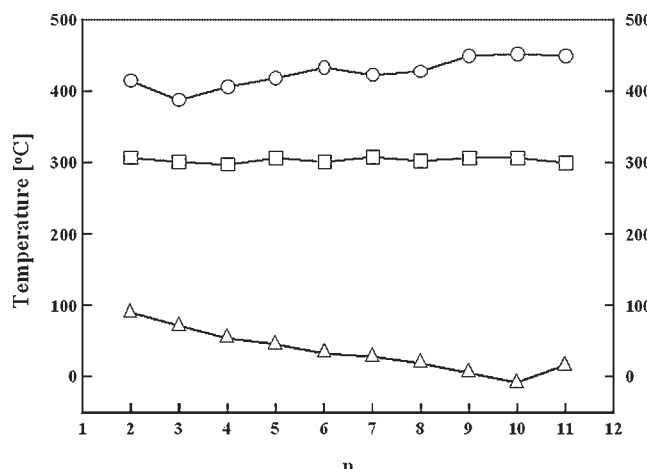


**Figure 4.** Alkyl chain length ( $n$ ) dependence on thermal properties (○): degradation, (□): conversion, (△): glass transition temperatures

because the glass transition temperature is much lower than the conversion temperature.

Figure 5a shows the isothermal decomposition behaviors for 2,9-dihexylpentacene precursor in nitrogen atmosphere at normal pressure at various temperatures. These decay curves converged to the theoretical value (about 72%), indicating that no side reactions or decomposition reactions occurred during

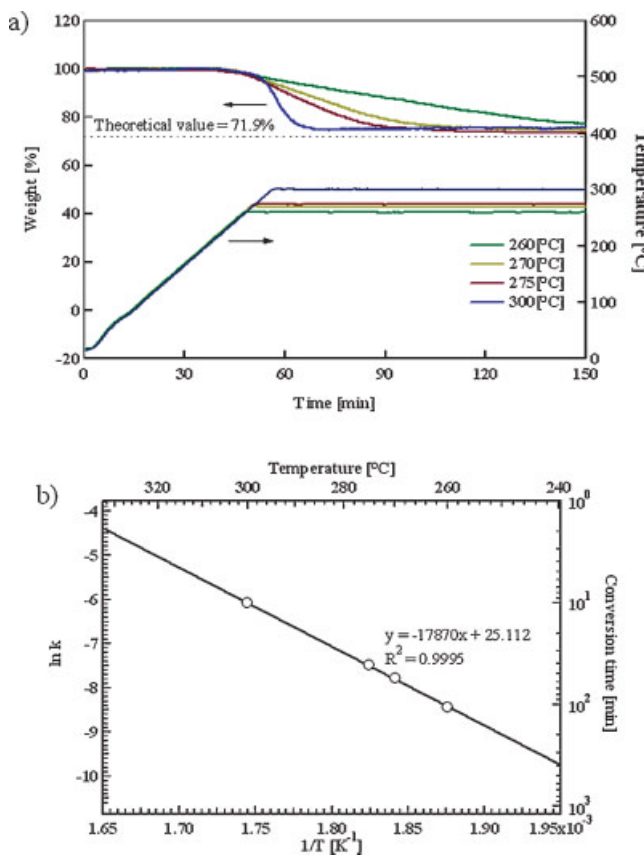


**Figure 5.** Isothermal decomposition behaviors for 2,9-dihexylpentacene precursor in nitrogen atmosphere at normal pressure (a), and Arrhenius plot for the decomposition rate (b).

and/or after desired retro-Diels–Alder reaction. The conversion rates were calculated by the slope of the decay curves at inflection points. Arrhenius plot for conversion rates is shown in Fig. 5b. Linear relationship was obtained between the logarithm of the rate constant and the reciprocal of conversion temperature. The apparent activation energy was calculated from the Arrhenius equation ( $k = Ae^{-E_a/RT}$ , where  $k$  is the rate constant,  $A$  is the frequency factor,  $E_a$  is the activation energy,  $R$  is the gas constant, and  $T$  is the absolute temperature). Activation energy  $E_a$  is estimated to be 149 kJ mol<sup>-1</sup>.

### Characterization of converted films

Figure 6 shows FT-IR spectra of 2,9-dihexylpentacene precursor (a), the precursor annealed at 300°C for 3 h (b), annealed film washed with chloroform (c), and original 2,9-dihexylpentacene (d). FT-IR spectrum of the precursor (Fig. 6a) shows the characteristic peak of C=O stretching bands at 1704 and 1748 cm<sup>-1</sup>. After annealing (Fig. 6b), the peak at 910 cm<sup>-1</sup> was observed, which is characteristic of 2,9-dihexylpentacene (Fig. 6d). These results indicate that the precursor was smoothly converted to dialkylpentacene. As shown in Fig. 6b, however, small peaks were observed in the carbonyl region, indicating that a small amount of residual precursor, and/or generated azocarboxylate exist just after annealing. Fig. 6c indicates that impurities were easily removed by washing the annealed film with toluene. Because of the low solubility of the regenerated 2,9-dihexylpentacene, negligible amount of dihexylpentacene is expected to be washed away in this process. In UV-Vis spectrum of the annealed film, characteristic absorptions (in solid state) at

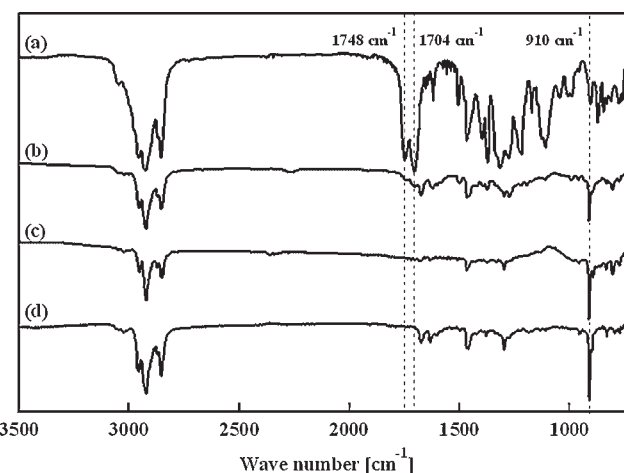


**Figure 6.** FT-IR spectra of 2,9-dihexylpentacene precursor (a), the precursor annealed at 300°C for 30 min (b), the annealed film washed with chloroform (c), and 2,9-dihexylpentacene (d)

542, 583, 620, 651, 683 nm were observed, which also confirmed that dialkylpentacene was regenerated by annealing.

Figure 7 shows microscope images of thin films of 2,9-dihexylpentacene regenerated by the annealing of precursor film deposited on a KBr substrate at 300°C for 30 min in nitrogen atmosphere. From optical microscope images (Fig. 7a and b), it is revealed that the color of films was changed from inherently colorless to blue on annealing. No clear-cut boundaries between domains were observed from POM images (Fig. 7c and d). After

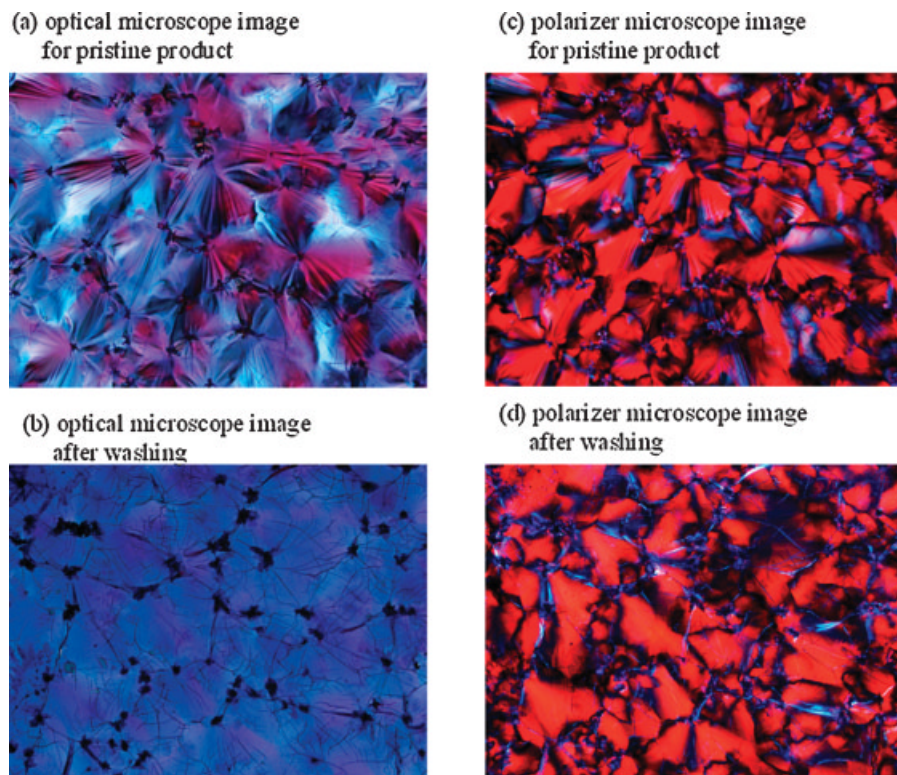


**Figure 7.** Optical microscope (a), (b) and polarizer microscope (c), (d) images of thin films of regenerated 2,9-dihexylpentacene deposited on a KBr substrate after annealing at 300°C for 30 min. (a) and (c): for pristine product just after thermal treatment, (b) and (d): the films washed with toluene.

annealing at 300°C, the films are gradually cooled. During the process, the regenerated 2,9-dihexylpentacene passed through the ordered smectic phase (crystal-smectic; 95°C, smectic-isotropic; 182°C<sup>[11]</sup>). It is possible for regenerated 2,9-dihexylpentacene to form liquid crystal glass as well as normal crystal. Significant difference was not observed between the images before and after washing with toluene, indicating that the amount of impurities is very small, and resulting morphologies maintain in the washing process.

From Fig. 7, the domain size was in the range of 50–200 μm, which was larger than that of vacuum-deposited pentacene polycrystalline, which is reported to be about 5–10 μm.<sup>[18]</sup> The large domains afford high mobility for OFETs, and improve the process reproducibility in OFET device fabrication, since the channel length of device is generally designed in the range of 10–50 μm. The large domain would cover the channel with a monodomain and the best performance of the material would be expected.

## CONCLUSIONS

We synthesized Diels–Alder adducts of 2,9-dialkylpentacenes with diethyl azocarboxylate as precursors. As expected these precursors were almost miscible with organic solvents such as toluene, tetrahydrofuran, and chloroform. Precursor solution showed chemical stability in air at room temperature. 2,9-Dialkylpentacene was smoothly regenerated by annealing the precursor films at around 300°C via retro-Diels–Alder reaction. Conversion temperature was slightly dependent on the length of alkyl chains accompanied with the odd–even effect. From isothermal TGA, Arrhenius type of kinetics was observed for retro-Diels–Alder reaction, and the activation energy was estimated to 149 kJ mol<sup>-1</sup>. From microscope observation, the domain size of regenerated 2,9-dihexylpentacene was in the range of 50–200 μm. The large domain size would improve reproducibility in the fabrication of OFET devices and would afford high device performance. We are investigating the fabrication of solution-processed OTFTs utilizing reported Diels–Alder adducts as precursors and will report the device performance in the near future.

## EXPERIMENTAL

### General

All reagents were bought from Wako Pure Chemical Industries, Ltd. and used without further purification. Column chromatography was performed with silica gel 60 N (spherical, neutral), 63–210 μm bought from KANTO chemical Co., Inc. All compounds were characterized using a combination of MS spectroscopy (Shimazu, GCMS-QP2010), <sup>1</sup>H-NMR spectroscopy (NMR, Varian Mercury Plus 400 MHz), and IR spectroscopy (Shimazu, FTIR-8300).

### Synthesis

As shown in Fig. 1, Diels–Alder adducts for 2,9-dialkylpentacenes were synthesized based on the method described by Joung *et al.*<sup>[8]</sup> Starting materials, 2,9-dialkylpentacenes were synthesized based on the method described elsewhere.<sup>[11]</sup> For example, 2,9-dihexylpentacene precursor was synthesized as follows.

### Synthesis of Diels–Alder adduct for dihexylpentacene precursor (DEAD-C6)

A mixture of 2,9-dihexylpentacene (0.50 g, 1.12 mmol), 40% diethyl azodicarboxylate (DEAD) toluene solution (0.75 g, 1.73 mmol), and toluene (30 ml) was heated at 110°C for 3 h under a nitrogen atmosphere. The mixture was cooled to the room temperature and purified by column chromatography eluting with hexane/ethyl acetate (4/1), and dried to give 0.35 g (0.56 mmol) of light yellow powder (50%).

<sup>1</sup>H NMR (400 MHz, CDCl<sub>3</sub>, δ ppm): 0.85 (t, 6H), 1.10–1.22 (br, 6H), 1.22–1.36 (m, 12H), 1.64 (m, 4H), 2.72 (t, 4H), 4.14 (m, 4H), 6.47 (s, 2H), 7.30 (m, 2H), 7.54 (d, 2H), 7.66–7.73 (m, 4H), 7.84 (d, 2H). FT-IR (KBr): 3048, 2955, 2926, 2855, 1747, 1703, 1617, 1505, 1465, 1395, 1371, 1314, 1276, 1218, 1173, 1110, 1047, 1007, 991, 905, 871, 845, 832, 776, 759, 721, 637, 554 cm<sup>-1</sup>. MS (EI, 70 eV): *m/z* (%) = 620 (M<sup>+</sup>, 1), 448 (7), 447 (35), 446 (100), 377 (1), 376 (5), 375 (15), 305 (5), 304 (15), 153 (2).

### Synthesis of Diels–Alder adduct for diethylpentacene (DEAD-C2)

Light yellow powder (yield, 63%).

<sup>1</sup>H NMR (400 MHz, CDCl<sub>3</sub>, δ ppm): 1.12–1.26 (br, 6H), 1.29 (t, 6H), 2.76 (q, 4H), 4.17 (m, 4H), 6.51 (s, 2H), 7.32 (m, 2H), 7.58 (s, 2H), 7.71 (d, 2H), 7.70–7.79 (s, 2H), 7.86 (d, 2H). FT-IR (KBr): 3048, 2964, 2933, 2873, 1747, 1701, 1617, 1503, 1465, 1395, 1371, 1314, 1276, 1218, 1172, 1110, 1053, 1007, 991, 905, 871, 845, 819, 772, 696, 636, 553 cm<sup>-1</sup>. MS (EI, 70 eV): *m/z* (%) = 508 (M<sup>+</sup>, 2), 336 (4), 335 (28), 334 (100), 321 (1), 320 (4), 319 (15), 305 (3), 304 (10), 152 (3).

### Synthesis of Diels–Alder adduct for dipropylpentacene (DEAD-C3)

Light yellow powder (yield, 49%).

<sup>1</sup>H NMR (400 MHz, CDCl<sub>3</sub>, δ ppm): 0.92 (t, 6H), 1.10–1.20 (br, 6H), 1.67 (m, 4H), 2.67 (t, 4H), 4.12 (m, 4H), 6.47 (s, 2H), 7.29 (m, 2H), 7.54 (d, 2H), 7.70 (m, 2H), 7.70–7.74 (s, 2H), 7.84 (d, 2H). FT-IR (KBr): 3049, 2956, 2931, 2870, 1747, 1703, 1617, 1506, 1465, 1395, 1371, 1314, 1275, 1220, 1172, 1110, 1041, 1007, 991, 908, 870, 845, 771, 694, 637, 553 cm<sup>-1</sup>. MS (EI, 70 eV): *m/z* (%) = 536 (M<sup>+</sup>, 2), 364 (5), 363 (30), 362 (100), 335 (1), 334 (4), 333 (14), 305 (3), 304 (12), 152 (2).

### Synthesis of Diels–Alder adduct for dibutylpentacene (DEAD-C4)

Light yellow powder (yield, 46%).

<sup>1</sup>H NMR (400 MHz, CDCl<sub>3</sub>, δ ppm): 0.90 (t, 6H), 1.10–1.20 (br, 5H), 1.34 (m, 4H), 1.63 (m, 4H), 2.72 (t, 4H), 4.12 (m, 4H), 6.47 (s, 2H), 7.30 (m, 2H), 7.54 (d, 2H), 7.66–7.74 (m, 4H), 7.84 (d, 2H). FT-IR (KBr): 3049, 2956, 2929, 2857, 1748, 1701, 1617, 1506, 1465, 1395, 1371, 1314, 1275, 1218, 1172, 1109, 1045, 1008, 990, 906, 871, 845, 831, 813, 775, 759, 694, 637, 553 cm<sup>-1</sup>. MS (EI, 70 eV): *m/z* (%) = 564 (M<sup>+</sup>, 1), 392 (6), 391 (33), 390 (100), 349 (1), 348 (5), 347 (16), 305 (5), 304 (14), 153 (2).

### Synthesis of Diels–Alder adduct for dipentylpentacene (DEAD-C5)

Light yellow powder (yield, 51%).

<sup>1</sup>H NMR (400 MHz, CDCl<sub>3</sub>, δ ppm): 0.87 (t, 6H), 1.10–1.22 (br, 6H), 1.31 (s, 8H), 1.66 (m, 4H), 2.73 (t, 4H), 4.15 (m, 4H), 6.48 (s, 2H), 7.31

(m, 2H), 7.56 (d, 2H), 7.68–7.76 (s, 4H), 7.85 (d, 2H). FT-IR (KBr): 3047, 2957, 2930, 2856, 1747, 1705, 1618, 1504, 1466, 1396, 1371, 1315, 1275, 1219, 1173, 1109, 1043, 1007, 991, 906, 872, 845, 771, 759, 694, 638, 553  $\text{cm}^{-1}$ . MS (EI, 70 eV):  $m/z$  (%) = 592 ( $M^+$ , 2), 420 (6), 419 (35), 418 (100), 363 (1), 362 (5), 361 (16), 305 (5), 304 (14), 153 (2).

### Synthesis of Diels–Alder adduct for diheptylpentacene (DEAD-C7)

Light yellow powder (yield, 48%).

$^1\text{H}$  NMR (400 MHz,  $\text{CDCl}_3$ ,  $\delta$  ppm): 0.84 (t, 6H), 1.10–1.22 (br, 6H), 1.22–1.35 (m, 8H), 1.64 (m, 4H), 2.71 (t, 4H), 4.12 (m, 4H), 6.46 (s, 2H), 7.29 (m, 2H), 7.54 (d, 2H), 7.67–7.73 (m, 4H), 7.84 (d, 2H). FT-IR (KBr): 3049, 2955, 2928, 2855, 1749, 1701, 1618, 1504, 1466, 1396, 1371, 1315, 1277, 1219, 1173, 1111, 1043, 1009, 991, 904, 872, 845, 771, 721, 638, 554  $\text{cm}^{-1}$ . MS (EI, 70 eV):  $m/z$  (%) = 648 ( $M^+$ , 2), 476 (8), 475 (37), 474 (100), 391 (1), 390 (6), 389 (15), 305 (4), 304 (12), 153 (2).

### Synthesis of Diels–Alder adduct for dioctylpentacene (DEAD-C8)

Light orange oil (yield, 58%).

$^1\text{H}$  NMR (400 MHz,  $\text{CDCl}_3$ ,  $\delta$  ppm): 0.84 (t, 6H), 1.10–1.22 (br, 6H), 1.18–1.35 (m, 20H), 1.64 (m, 4H), 2.71 (t, 4H), 4.12 (m, 4H), 6.47 (s, 2H), 7.30 (m, 2H), 7.54 (d, 2H), 7.66–7.74 (m, 4H), 7.84 (d, 2H). FT-IR (KBr): 3049, 2956, 2925, 2854, 1751, 1700, 1617, 1503, 1466, 1395, 1371, 1313, 1275, 1219, 1173, 1109, 1043, 1008, 991, 904, 871, 845, 832, 811, 771, 759, 721, 637, 553  $\text{cm}^{-1}$ . MS (EI, 70 eV):  $m/z$  (%) = 676 ( $M^+$ , 2), 504 (8), 503 (41), 502 (100), 405 (1), 404 (5), 403 (13), 305 (4), 304 (11), 152 (1).

### Synthesis of Diels–Alder adduct for dinonylpentacene precursor (DEAD-C9)

Light orange oil (yield, 53%).

$^1\text{H}$  NMR (400 MHz,  $\text{CDCl}_3$ ,  $\delta$  ppm): 0.85 (t, 6H), 1.10–1.20 (br, 6H), 1.18–1.35 (m, 24H), 1.64 (m, 4H), 2.71 (t, 4H), 4.12 (m, 4H), 6.47 (s, 2H), 7.30 (m, 2H), 7.54 (d, 2H), 7.66–7.75 (m, 4H), 7.84 (d, 2H). FT-IR (KBr): 3044, 2956, 2925, 2854, 1751, 1701, 1617, 1502, 1465, 1395, 1371, 1313, 1275, 1220, 1173, 1109, 1043, 1008, 991, 905, 871, 845, 811, 775, 759, 721, 637, 553  $\text{cm}^{-1}$ . MS (EI, 70 eV):  $m/z$  (%) = 704 ( $M^+$ , 2), 532 (9), 531 (42), 530 (100), 419 (1), 418 (4), 417 (11), 305 (3), 304 (8), 152 (1).

### Synthesis of Diels–Alder adduct for didecylpentacene (DEAD-C10)

Light orange powder (yield, 43%).

$^1\text{H}$  NMR (400 MHz,  $\text{CDCl}_3$ ,  $\delta$  ppm): 0.85 (t, 6H), 1.10–1.22 (br, 6H), 1.18–1.35 (m, 28H), 1.64 (m, 4H), 2.71 (t, 3H), 4.12 (m, 4H), 6.46 (s, 2H), 7.30 (m, 2H), 7.54 (d, 2H), 7.66–7.76 (m, 4H), 7.84 (d, 2H). FT-IR (KBr): 3049, 2955, 2926, 2853, 1747, 1705, 1618, 1504, 1466, 1396, 1371, 1315, 1277, 1219, 1173, 1109, 1043, 1007, 989, 903, 872, 845, 771, 721, 638, 554  $\text{cm}^{-1}$ . MS (EI, 70 eV):  $m/z$  (%) = 733 ( $M^+$ , 1), 560 (11), 559 (45), 558 (100), 433 (1), 432 (5), 431 (12), 305 (4), 304 (10), 153 (1).

### Synthesis of Diels–Alder adduct for diundecylpentacene (DEAD-C11)

Light orange powder (yield, 37%).

$^1\text{H}$  NMR (400 MHz,  $\text{CDCl}_3$ ,  $\delta$  ppm): 0.85 (t, 6H), 1.10–1.22 (br, 6H), 1.18–1.35 (m, 32H), 1.64 (m, 4H), 2.71 (t, 4H), 4.13 (m, 4H), 6.47 (s, 2H), 7.30 (m, 2H), 7.54 (d, 2H), 7.66–7.76 (m, 4H), 7.84 (d, 2H). FT-IR (KBr): 3049, 2954, 2925, 2853, 1751, 1706, 1617, 1506, 1465, 1395, 1371, 1314, 1275, 1218, 1172, 1109, 1045, 1008, 991, 903, 872, 845, 832, 811, 771, 759, 720, 636, 553  $\text{cm}^{-1}$ . MS (EI, 70 eV):  $m/z$  (%) = 760 ( $M^+$ , 2), 588 (11), 587 (49), 586 (100), 447 (1), 446 (4), 445 (10), 305 (3), 304 (7), 153 (1).

### Thermal analysis and optical microscope observation

The thermal transition of Diels–Alder adducts was investigated by differential scanning calorimetry (DSC, TA Instruments Q10) under nitrogen flow. The retro-Diels–Alder reaction behavior was monitored by thermogravimetric analysis (TG, ULVAC-RIKO, Inc. VAP-9000). Optical microscope observation was carried out with polarizing optical microscopy (POM, Nikon E600 POL).

### REFERENCES

- [1] C. D. Dimitrakopoulos, P. R. L. Malenfant, *Adv. Mater.* **2002**, *14*, 99–117.
- [2] J. Naciri, J. Y. Fang, M. Moore, D. Shenoy, C. S. Dulcey, R. Shashidhar, *Chem. Mater.* **2000**, *12*, 3288–3295.
- [3] M. M. Payne, S. R. Parkin, J. E. Anthony, C. C. Kuo, T. N. Jackson, *J. Am. Chem. Soc.* **2005**, *127*, 4986–4987.
- [4] H. Meng, M. Bendikov, G. Mitchell, R. Helgeson, F. Wudl, Z. Bao, T. Siegrist, C. Kloc, C. H. Chen, *Adv. Mater.* **2003**, *15*, 1090–1093.
- [5] P. T. Herwig, K. Müllen, *Adv. Mater.* **1999**, *11*, 480–483.
- [6] H. Uno, Y. Yamashita, M. Kikuchi, H. Watanabe, H. Yamada, T. Okujima, T. Ogawa, N. Ono, *Tetrahedron Lett.* **2005**, *46*, 1981–1983.
- [7] K. Y. Chen, H. H. Hsieh, C. C. Wu, J. J. Hwang, T. J. Chow, *Chem. Commun.* **2007**, 1065–1067.
- [8] M. J. Joung, J. H. Ahn, S. Y. Kang, K. H. Baek, S. D. Ahn, L. M. Do, C. A. Kim, G. H. Kim, I. K. You, S. M. Yoon, K. S. Suh, *Bull. Korean. Chem. Soc.* **2003**, *24*, 1862–1864.
- [9] K. P. Weidkamp, A. Afzali, R. M. Tromp, R. J. Hamers, *J. Am. Chem. Soc.* **2004**, *126*, 12740–12741.
- [10] A. Afzali, C. D. Dimitrakopoulos, T. L. Breen, *J. Am. Chem. Soc.* **2002**, *124*, 8812–8813.
- [11] K. Okamoto, T. Kawamura, M. Sone, K. Ogino, *Liq. Cryst.* **2007**, *34*, 1001–1007.
- [12] A. M. van de Craats, N. Stutzmann, O. Bunk, M. M. Nielsen, M. Watson, K. Müllen, H. D. Chanzy, H. Sirringhaus, R. H. Friend, *Adv. Mater.* **2003**, *15*, 495–499.
- [13] A. J. J. M. van Breemen, P. T. Herwig, C. H. T. Chlon, J. Sweelssen, H. F. M. Schoo, S. Setayesh, W. M. Hardeman, C. A. Martin, D. M. de Leeuw, J. J. P. Valetton, C. W. M. Bastiaansen, D. J. Broer, A. R. Popa-Merticau, S. C. J. Meskers, *J. Am. Chem. Soc.* **2006**, *128*, 2336–2345.
- [14] H. Sirringhaus, R. J. Wilson, R. H. Friend, M. Inbasekaran, W. Wu, E. P. Woo, M. Grell, D. C. Bradley, *Appl. Phys. Lett.* **2000**, *77*, 406–408.
- [15] Y. Wu, P. Liu, B. S. Ong, T. Srikumar, N. Zhao, G. Botton, S. P. Zhu, *Appl. Phys. Lett.* **2005**, *86*, 142102.
- [16] I. McCulloch, M. Heeney, C. Bailey, K. Geneviev, I. Macdonald, M. Shkunov, D. Sparrowe, S. Tierney, R. Wagner, W. Zhang, M. L. Chabinyc, R. J. Kline, M. D. McGehee, M. F. Toney, *Nat. Mater.* **2006**, *5*, 328–333.
- [17] J. E. Anderson, J. M. Lehn, *Tetrahedron* **1968**, *24*, 123–135.
- [18] T. Minari, T. Nemoto, S. Isoda, *J. Appl. Phys.* **2006**, *99*, 034506.